VERSITA

Central European Journal of **Physics**

Low temperature measurements by infrared spectroscopy in CoFe$_2$O$_4$ ceramic

Renata Bujakiewicz-Korońska[1*], Łukasz Hetmańczyk[2,3], Barbara Garbarz-Glos[1],
Andrzej Budziak[4], Anna Kalvane[5], Karlis Bormanis[5], Kacper Drużbicki[2,3]

1 Pedagogical University, Institute of Physics, Podchorazych 2, 30-084 Krakow, Poland

2 Jagiellonian University, Faculty of Chemistry, Ingardena 3, 30-060 Krakow, Poland

3 Frank Laboratory of Neutron Physics, Joint Institute for Nuclear Research, 141980 Dubna, Russia

4 The H. Niewodniczanski Institute of Nuclear Physics PAN, Radzikowskiego 152, 31-342 Krakow, Poland

5 Institute of Solid State Physics, University of Latvia, Kengeraga 8, LV-1063, Riga, Latvia

Abstract: This paper presents results of new far-infrared and middle-infrared measurements (wavenumber range of
4000 - 100 cm^{-1}) of the CoFe$_2$O$_4$ ceramic in the temperature range from 300 K to 8 K. The band positions
and their shapes remain constant across the wide temperature range. The quality of the sample was
investigated by X-ray, EDS and EPMA studies. The CoFe$_2$O$_4$ retains the cubic structure ($Fd-3m$) across
the temperature range from 85 K to 360 K without any traces of distortion. Based on current knowledge
the polycrystalline CoFe$_2$O$_4$ does not exhibit any phase transitions across the temperature range from 8 K
to 300 K.

PACS (2008): 78.30.-j

Keywords: infrared • FT-FIR • FT-MIR • CoFe$_2$O$_4$ • cobalt spinel ferrite

© Versita sp. z o.o.

1. Introduction

Cobalt spinel ferrite CoFe$_2$O$_4$ (CFO) is interesting due
to its structural, magnetic, and electrical properties. It
has a Curie temperature around 793 K, strong magnetic
anisotropy, high moderate saturation magnetisation and
coercivity, and high mechanical hardness. These proper-
ties, combined with the material's physical and chemical
stability make it suitable for magnetic recording applica-
tions [1–6].

Cobalt ferrite has been extensively investigated. Raman
and IR spectra for CFO were obtained in the wavenum-
ber range (800 – 200) cm^{-1} across the temperature range
(300 – 870) K by Yu *et al.* [7] and in the range (900 –
100) cm^{-1} at room temperature (RT) by Wang *et al.* [8].
The aim of this work is to study the low temperature de-
pendence of far–infrared (FIR) and middle–infrared (MIR)
spectra in the range (4000 – 100) cm^{-1}.

*E–mail: rbk@up.krakow.pl

2. Experiment and results

2.1. Sample preparation

The CFO samples were made by the following conventional method. CoFe$_2$O$_4$ powder was obtained by solid phase synthesis from Co$_2$O$_3$-99,5 % and Fe$_2$O$_3$-70 % oxides. The starting materials were weighed according to the chemical formula, homogenized and milled in an agate ball–mortar in ethanol for 24 h, dried and calcined for 1 h at a temperature of 1000 K. The calcined powders were then reground, pressed under a pressure of 15 MPa, and sintered for 4 hours at 1100 K.

2.2. X-ray investigations

X-ray studies were carried out using an X'Pert PRO (PANalytical) diffractometer with a CuK$_\alpha$ radiation and a graphite monochromator. The temperature of the CFO sample was stabilized (accuracy ±1 K) by means of a TTK 450 low temperature chamber. The measurements were performed during heating. After each heating stage the sample was held for about 10min to reach temperature equilibrium. A profile–fitting program, FULLPROF [9], based on the Rietveld method was used to analyze and fit the spectra. An exemplary diagram of X–ray measurements taken at RT is presented in Fig.1a and the obtained lattice parameter $a = 8.385$ agrees with data in [10]. The CFO sample maintained a cubic structure ($Fd-3m$) across the whole temperature range of (85 - 360) K without any traces of distortion. The lattice parameter increased from 8.3757 at 85 K up to 8.3901 at 360 K (Fig. 1b), which corresponds to a change of the unit cell volume of ~ 0.5 %. Cations of Co and Fe occupy 8a and 16d special Wyckoff positions at (1/2, 1/2, 1/2) and (1/8, 1/8, 1/8), respectively. Oxygen ions occupy the 32e positions at (x, x, x). The obtained value $x = 0.2555(8)$ at RT agrees with data from [11]. Typical reliability factors obtained from refinements of the x-ray diffraction (XRD) patterns were: R$_p \sim$ 12, R$_{wp} \sim$ 15, R$_{wp} \sim$ 6 and Chi$^2 \sim$ 5.5.

2.3. Morphological and chemical investigations

The ceramic microstructure was investigated by means of an electron scanning microscope with a Noran–Vantage microanalyses system. Scanning Electron Microscopy (SEM) micrographs of the fractured surface of the CFO sample with magnifications of 500×, 1000×, and 30000× are presented in Fig. 2. The microphotographs of fractures of CFO showed that the sample was perfectly sintered and dense (95 % theoretical). The fractures were fragile in na-

Table 1. Values of the elastic parameters of CFO.

ρ [kg/m^3]	E [GPa]	G [GPa]	v
6260 ± 100	174.5 ± 16.6	66.8 ± 0.2	0.307 ± 0.014

ture and crystalline structures were observed within the grains. The average grain size (measured by the linear intercept method) was 300 nm. The homogeneity of element distribution in the samples was confirmed by the Electron Probe Micro-Analysis (EPMA) method using an X-ray microprobe.

2.4. Elastic properties

Three material constants: the Young's modulus E, the shear modulus G and the Poisson ratio v, were determined based on investigations of the elastic properties of the CFO polycrystalline samples. An ultrasonic method was used and the measurements were taken with an INCO –VERITAS Ultrasonic Measuring Set UZP-1. Two kinds of transducers were used: 10 MHz transducers, connected to a sample by oil, were used for longitudinal waves while 2 MHz transducers, stuck on a sample with Canada balsam, were applied for transverse waves. Material constants were calculated from longitudinal and transverse ultrasonic wave propagation velocity and the apparent density of samples using the following formulas [12, 13]:

$$E = V_L^2 \rho (1 + v)(1 - 2v)/(1 - v),$$

$$G = V_T^2 \rho,$$

$$v = (V_L^2 - 2V_T^2)/(2V_L^2 - 2V_T^2),$$

where: ρ - density, V_L - velocity of longitudinal wave, V_T - velocity of transverse wave. V_L was measured at 6189.4 m/s, and V_T at 3265.9 m/s. The material constants measured in the plane direction of the CFO ceramic are given in Table 1. The CFO sample had a high density and small porosity therefore the material constants are slightly different to those in [10]. These results confirm the high mechanical hardness of CFO.

2.5. FT-FIR and FT-MIR studies

The FIR and MIR infrared absorption measurements were performed using a Bruker 70v vacuum Fourier Transform spectrometer. The transmission spectra were measured with a resolution of 2 cm^{-1} and using 32 scans per spectrum. The FIR spectra (600-80) cm^{-1} were collected with the sample suspended in apiezon N grease and placed on a polyethylene disc. The MIR spectra (4000 - 400) cm^{-1}
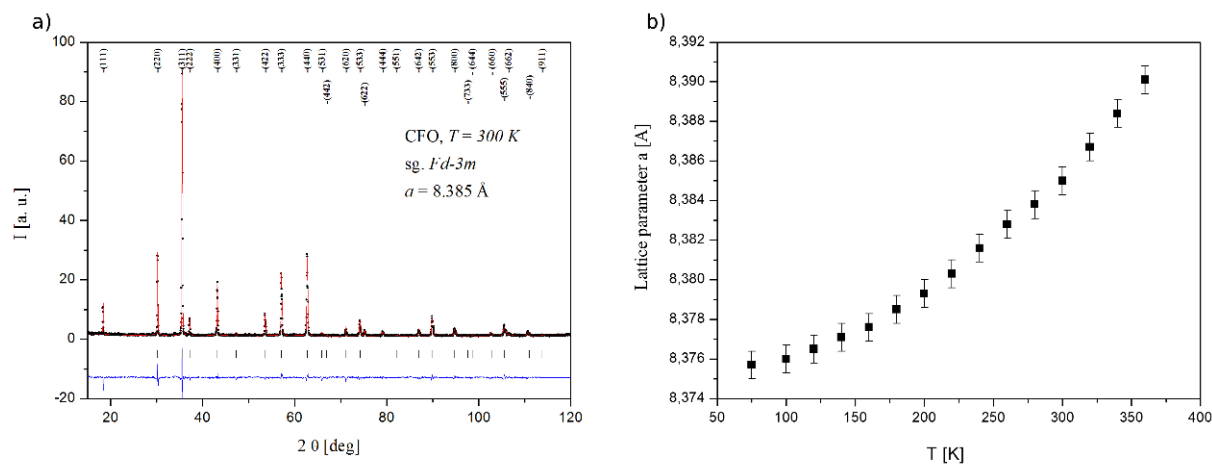
Figure 1. a) X-ray diffraction pattern of the CFO ceramic at RT. Upper tick marks indicate the position of the Bragg reflections for the cubic phase (*Fd-3m*); only the strongest ones are described. b) The unit cell parameter a of the cubic phase (*Fd-3m*) for the CFO as a function of temperature.
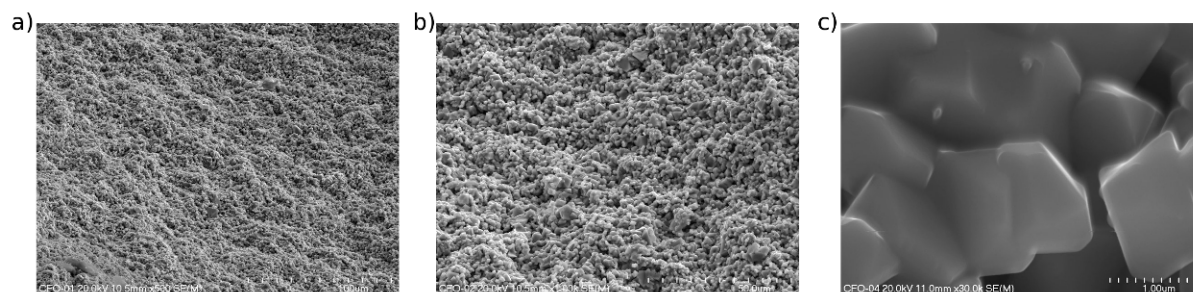
Figure 2. SEM micrographs of the fractured surface of the CFO sample. Magnif.: a) 500×, b)1000×, c) 30000×.

were measured with the sample mixed with dry KBr and pressed into a pellet and placed on a KRS window.

The samples were loaded into a cryostat DE–202A at room temperature and measurements were taken during the cooling process down to ca. 8 K with a cooling rate of 3 K/min. The desired temperature was measured with an accuracy of 0.1 K and stabilized for ca. 3 minutes before the data was recorded. A LakeShore 331S temperature controller equipped with a diode sensor was used to control the temperature.

Fig. 3a presents selected MIR spectra in the range (4000 – 450) cm^{-1}. One intense maximum is found at ca. 590 cm^{-1}, which can be seen, from the lower wavenumbers, as a shoulder of the main band. No changes are vissible in peak position or band shape (full width at half maximum) across the temperature range. Raman spectra were recorded and interpreted by Wang and Ren [8], T. Yu *et al.* [14] and P. Chandramohan *et al.* [15]. Fig. 3b shows selected MIR spectra in the range (1000 – 450) cm^{-1}

where the presence of the shoulder band is clearly visible. Fig. 3c shows selected FIR spectra of the CFO compound where a very weak and broad absorption band can be observed at 467 cm^{-1}. The next intense and broad band is visible at ca. 400 cm^{-1} with a shoulder band at ca. 345 cm^{-1}. Very weak and broad bands at ca. 230 cm^{-1} and ca 180 cm^{-1} are also visible. Once again the band positions and shapes are the same across the wide temperature range.

The bands at 590 cm^{-1} and 467 cm^{-1} are Raman active modes which are consistent with 575.5 cm^{-1} [15] and 470 cm^{-1} [8, 14, 15]. There are also four infrared active modes F_{1u} (400 cm^{-1}, 345 cm^{-1}, 230 cm^{-1}, 180 cm^{-1}). These low frequency modes can be assigned to vibrations of the tetrahedral sublattice, whereas the higher energy phonon mode at 590 cm^{-1} is probably connected with vibrations of the octahedral sublattice [8].
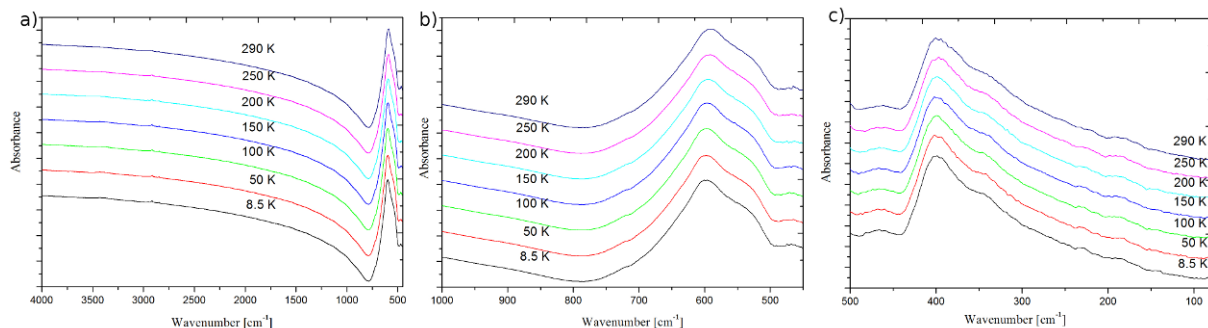
Figure 3. Selected spectra for CFO a) FT-MIR (4000-450) cm^{-1}, b) FT-MIR (1000-450) cm^{-1}, c) FT-FIR (500-80) cm^{-1}.

3. Calculations

3.1. *Ab initio* calculations

Periodic Boundary Condition (PBC) calculations of the phonon frequencies were performed with CASTEP code as implemented in Materials Studio 5.5[1] [16] and Generalized Gradient Approximation (GGA) represented by PBE functional [17, 18]. The computations were performed with a Troullier–Martins type Norm–Conserving (NC) pseudopotential developed by Bennett and Rappe[2] with a Plane–Wave kinetic energy cut-off of 750 eV. Initially, the unit cell consisted of 56 atoms in the well known cubic spinel structure (space group $= Fd - 3m$; $a_0 = 8.385$), constructed as presented in Fig. 4a. In the next step the unit cell was reduced to the Co$_2$Fe$_4$O$_8$ primitive cell of face-centered cubic. The resultant lattice parameters were fixed during the optimization and the delocalized internals were relaxed with 5.0×10^{-7} eV/atom; 5.0×10^{-3} eV/ and 5.0×10^{-3} convergence criteria for energy; Hellman–Feyman forces and atomic displacements, respectively. The electronic energy was calculated within the precise (54×54×54) FFT grid using a 5×5×5 Monkhorst–Pack grid for the Brillouin–zone sampling. A SCF tolerance of 5.0×10^{-10} eV/atom was applied along with electron smearing of 0.1 eV. The resultant equilibrium structure is presented in Fig. 4b. Finally, the calculations were also repeated under the same conditions with the full size unit cell presented in Fig. 4a.

---

[1] *Materials Studio 5.5, Accelrys Software Inc. ©, 2001–2011*

[2] *Andrew M. Rappe, Joseph W. Bennett, http://opium.sourceforge.net/ http://www.sas.upenn.edu/rappegroup/htdocs/Research/ psp_gga.html*

Since the structure studied is not an insulator it was impossible to simulate the IR activities via the linear-response approach. Also, applying the Hubbard correction to the phonon calculations, as may be suggested for the system under study, is impossible using curently available solid state DFT software. Hence, the numerical finite–displacement approach, as implemented in CASTEP, was applied to calculate the phonon modes at the Γ point as seen by vibrational optical spectroscopy. The Acoustic Sum Rule (ASR) was applied to the calculated frequencies. No imaginary frequencies were presented in the calculated results. It should be noted that the ultrasoft pseudopotentials along with pure LDA approach were also tested, however, no improvement was found.

3.2. Vibrational analysis

According to group theory, the irreducible representations for the studied systems are as follows:

$$\Gamma_{red} = A_{1g} + E_g + T_{1g} + 3T_{2g} + 2A_{2u} + 2E_u + 5T_{1u} + 2T_{2u}.$$

Within the expected normal modes, only the T_1u type vibrations are infrared–active, while A_{1g}, E_g and T_{2g} symmetry modes are visible in Raman spectroscopy. All the IR–active vibrations are triply degenerated while the T_{1g}, A_{2u}, E_u and T_{2u} symmetry vibrations are silent. None of the modes may be observed by both infrared and Raman spectroscopy. As the complete unit cell consists of 56 atoms, 165 (3N–3) modes may be observed with optical vibrational spectroscopy. By using the primitive cell approach the computational problem was reduced to 39 modes which undergo further degeneracy upon expanding the system. However, the computations revealed that the calculations within the full–unit cell dimension mainly resulted in further splitting of the silent modes, with no significant influence on the optically active vibrations.
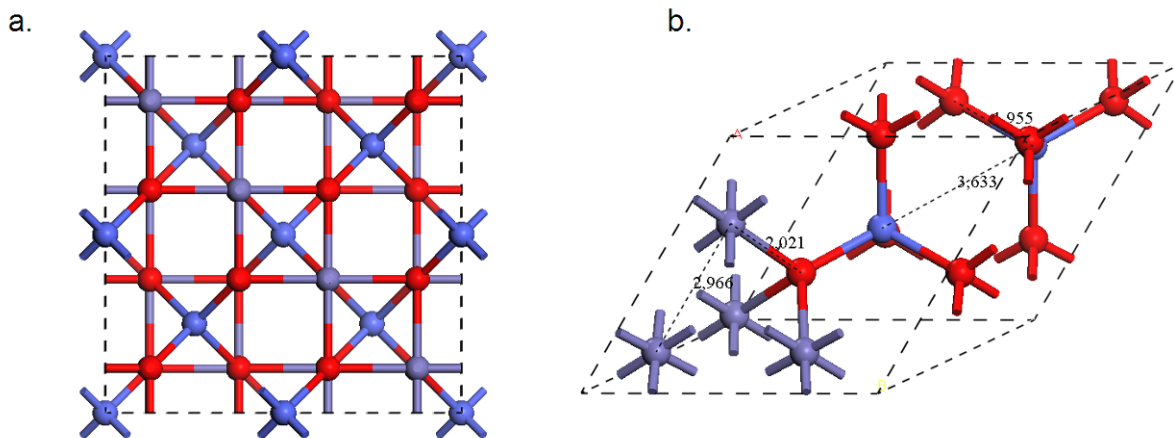
Figure 4. The constructed unit cell of $CoFe_2O_4$ a) along with the primitive cell, b) used for the vibrational analysis.
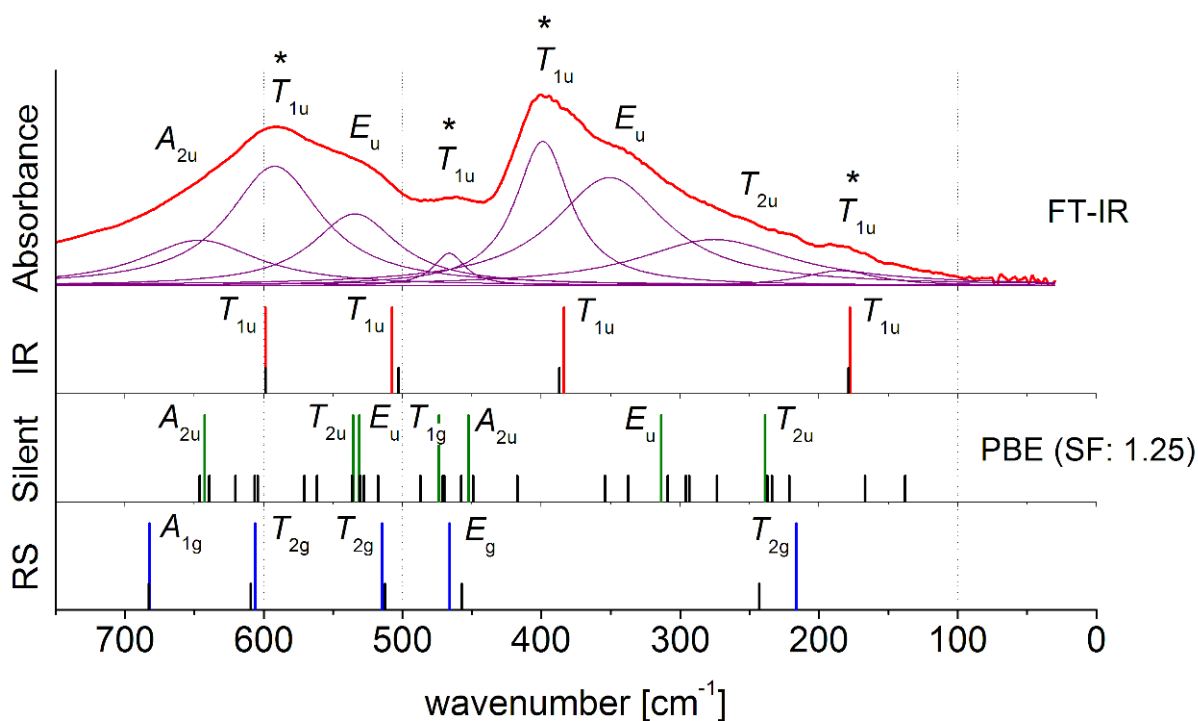
**Figure 5.** Experimental FT-IR spectrum of $CoFe_2O_4$ recorded at room temperature along with the theoretical frequencies of the IR- and RS-active and the silent modes. The higher sticks correspond to the primitive-cell model, while the lower ones come from the full unit cell approach. The main infrared bands are denoted with an asterisk. Note that the calculated frequencies have been multiplied by a factor of 1.25.

Fig. 5 compares the experimental room temperature FT–IR spectrum of the $CoFe_2O_4$ sample, with the calculated frequencies of the IR and Raman active modes and with the symmetry forbidden vibrations (silent modes). The higher sticks correspond to the primitive–cell model, while the lower ones are due to the full–unit cell approach. The infrared active T_{1u} type modes are shown in Fig. 6. The projection of all the calculated phonons has been given in the supplementary section.

All the theoretical frequencies fall into the far–infrared regime. The theory predicts four, triply degenerated
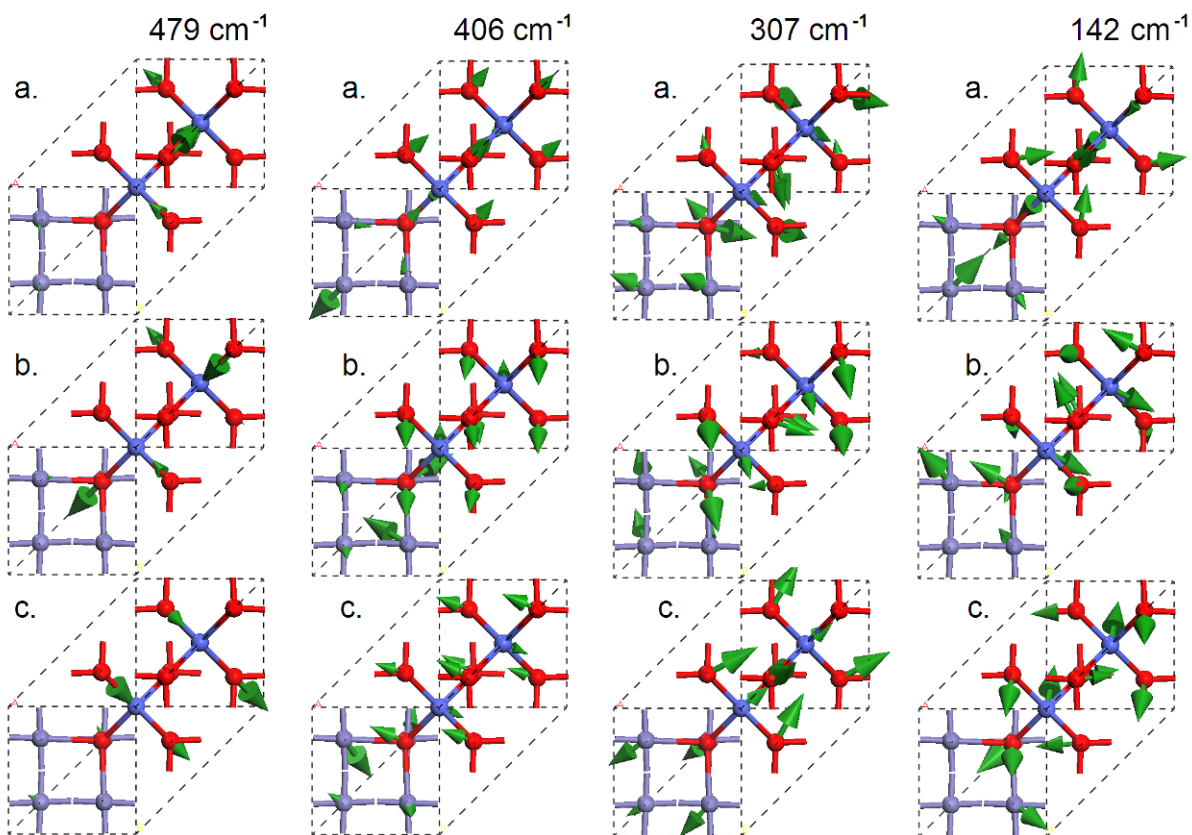
Figure 6. The infrared-active, triply-degenerated (a,b,c) T_{1u} type modes of $CoFe_2O_4$ primitive cell along with the corresponding frequencies calculated with PBE/NC/750 eV.

modes, observed at: 479, 406, 307 and 142 cm^{-1}. However, the experiment reveals more spectral features. Fig. 5 delivers the experimental spectrum deconvoluted with Lorentzian functions giving the following bands: 646, 592, 534, 466, 399, 351, 275 and 185 cm^{-1}. The calculated frequencies are strongly underestimated, by about 25%, with respect to the experiment. This effect may be partially linked with the insufficiency of the pure DFT in the description of such a strongly electron-correlated system. Although the results obtained suggest the need for introducing a better theoretical model, it allows for sufficient interpretation of the experimental features. Hence, the calculated frequencies have been empirically rescaled by a factor of 1.25. The computations suggest that the T_{1u} type modes may be assigned to the 592, 466, 399 and 185 cm^{-1} bands. The 534 and 351 cm^{-1} features seem to be the shoulders of the adjacent T_{1u} bands. Although the experimental spectrum may be disturbed by a modulated background, it is believed, that the remaining spectral features come from the activation of the A_{2u}, E_u and T_{2u} type silent modes, induced by a distortion of the structure which lowers the symmetry. However, the con-

sideration that the shoulder bands may also be related to a further resonance splitting of the main T_{1u} modes, due to some long-correlation effects, cannot be excluded.

4.   Conclusions

FT-MIR and FT-FIR measurements of CFO ceramic have been performed for the first time   across a wide temperature range.   In this paper, it is shown that CFO is a structurally stable compound in   temperatures from 8 K to 300 K. The small and large peaks of the bands are visible without changes across a wide temperature range. Moreover, no new bands with a wavenumber higher than 1000 cm^{-1} appear.   It follows that these types of measurements did not discover any phase transitions for the CFO ceramic which agrees with other data [10]. Interpretation of Raman spectra in the temperature range (300 – 870) K [14] of CFO particles [15], and single crystals [8] can be used in this case. The results obtained from the measurements of the lead-free $CoFe_2O_4$ ceramic suggest

the possibility of wide ranging practical applications of this material.

Acknowledgments

References

[1] V.K. Wadhawan, Introduction to ferroic materials (Gordon and Breach Science Publishers, The Netherlands, 2000)

[2] S.N. Okuno, S. Hashimoto, K. Inomata, J. Appl. Phys. 71, 5926 (1992)

[3] V. Pillai, D.O. Shah, J. Magn. Magn. Matter 163, 243 (1996)

[4] N. Moumen, P. Bonville, M.P. Pileni, J. Phys. Chem. 100, 14410 (1996)

[5] S. Ammar et al., J. Mater. Chem. 11, 186 (2001)

[6] B.H. Liu, J. Ding, Appl. Phys. Lett. 88, 042506 (2006)

[7] Y.-W. Ju, J.-H. Park, H.-R. Jung, S.-J. Cho, W.-J. Lee, Mater. Sci. Engin. B 147, 7 (2008)

[8] W.H. Wang, X. Ren, J. Cryst. Growth 289, 605 (2006)

[9] J. Rodriguez-Carvajal, Abstract Satelite Meeting on Powder Diffraction (Congr. Int. Union of Crystallography, Toulouse, 1990)

[10] Landolt–Börnstein, New Series III/4b (Springer, New York, 1970)

[11] R.W.G. Wyckoff, The second edition of Structure of Crystals (The Chemical Catalog Company, INC, New York 1931) 290

[12] W. Śmiga, B. Garbarz-Glos, Ferroelectrics 377, 137 (2008)

[13] J. Piekarczyk, H.W. Hennicke, R. Pampuch, cfi/Ber. D. K. G. 59, 227 (1982)

[14] T. Yu, Z. Shen, Y. Shi, J. Ding, J. Phys. Condens. Matter 14, L613 (2002)

[15] P. Chandramohan, M.P. Srinivasan, S. Velmurugan, S.V. Narasimhan, J. Sol. State Chem. 184, 89 (2011)

[16] S.J. Clark et al., Z. Kristallogr. 220, 567 (2005)

[17] J.P. Perdew, K. Burke, Y. Wang, Phys. Rev. B 54, 16533 (1996)

[18] J.P. Perdew, K. Burke, M. Ernzerhof, Phys. Rev. Lett. 77, 3865 (1996)